Ground-level spectroscopy analyses and classification of coral reefs using a hyperspectral camera

T. Caras & A. Karnieli

Coral Reefs
Journal of the International Society for Reef Studies

ISSN 0722-4028

Coral Reefs
DOI 10.1007/s00338-013-1033-1

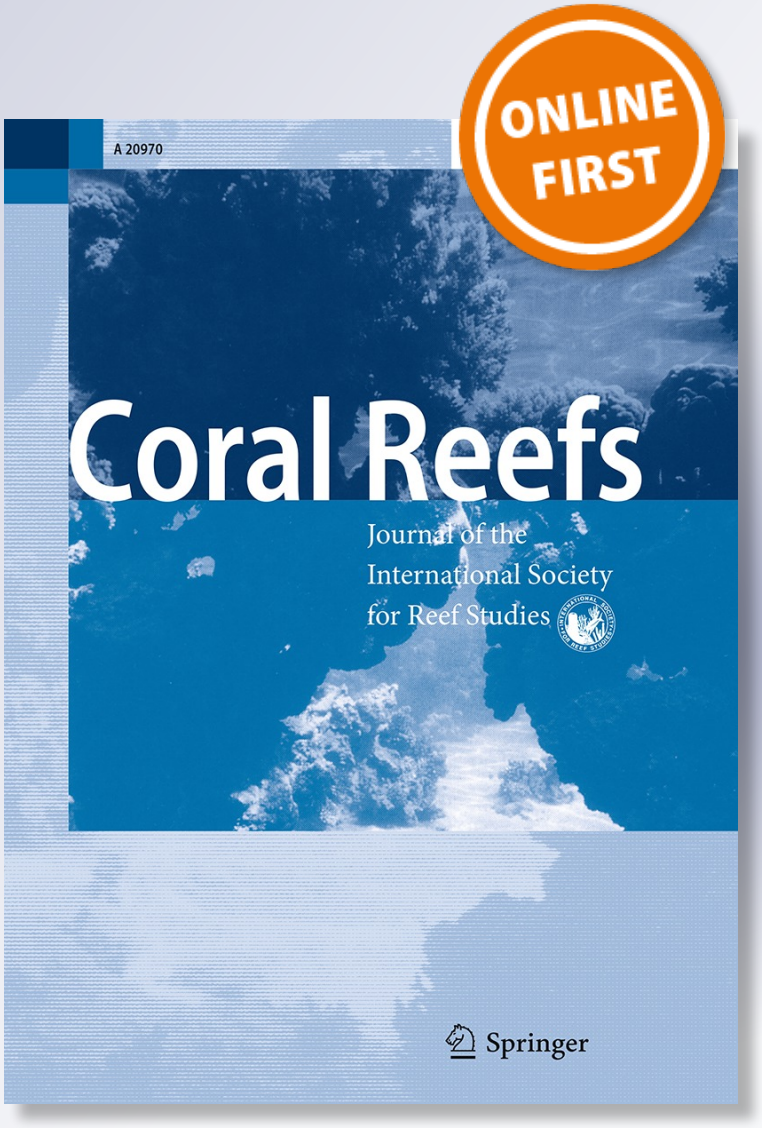

Springer

Coral Reefs
DOI 10.1007/s00338-013-1033-1

REPORT

Ground-level spectroscopy analyses and classification of coral reefs using a hyperspectral camera

T. Caras · A. Karnieli

Received: 16 May 2012 / Accepted: 15 March 2013

Abstract With the general aim of classification and mapping of coral reefs, remote sensing has traditionally been more difficult to implement in comparison with terrestrial equivalents. Images used for the marine environment suffer from environmental limitation (water absorption, scattering, and glint); sensor-related limitations (spectral and spatial resolution); and habitat limitation (substrate spectral similarity). Presented here is an advanced approach for ground-level surveying of a coral reef using a hyperspectral camera (400–1,000 nm) that is able to address all of these limitations. Used from the surface, the image includes a white reference plate that offers a solution for correcting the water column effect. The imaging system produces millimeter size pixels and 80 relevant bands. The data collected have the advantages of both a field point spectrometer (hyperspectral resolution) and a digital camera (spatial resolution). Finally, the availability of pure pixel imagery significantly improves the potential for substrate recognition in comparison with traditionally used remote sensing mixed pixels. In this study, an image of a coral reef table in the Gulf of Aqaba, Red Sea, was classified, demonstrating the benefits of this technology for the first time. Preprocessing includes testing of two normalization approaches, three spectral resolutions, and two spectral ranges. Trained classification was performed using support vector machine that was manually trained and tested against a digital image that provided empirical verification. For the classification of 5 core classes, the best results were achieved using a combination of a 450–660 nm spectral range, 5 nm wide bands, and the employment of red-band normalization. Overall classification accuracy was improved from 86 % for the original image to 99 % for the normalized image. Spectral resolution and spectral ranges seemed to have a limited effect on the classification accuracy. The proposed methodology and the use of automatic classification procedures can be successfully applied for reef survey and monitoring and even upscaled for a large survey.

Keywords Spectroscopy · Classification · Remote sensing · Hyperspectral · Glint · Monitoring · Survey

Introduction

Remotely sensed spectral data analysis has the potential to become a cost-effective practice for reef investigation, assessment, and monitoring (e.g., Mumby et al. 2004; Knudby et al. 2007; Collin and Planes 2012). The most desired application for remote sensing analysis of a coral reef is usually a basic classification (or thematic mapping), whereby the researcher wishes to quantify or map substrates in the study area (Johansen et al. 2008; Kendall and Miller 2008; Leiper et al. 2012). However, the integrity of remotely sensed results is often questionable as three main sources for errors obfuscate the image processing: (1) Analysis of marine habitats is confounded by the optical effect of the water and air columns above the substrate of interest (e.g., Pope and Fry 1997; Holden and LeDrew 2000; Hedley et al. 2010); (2) spatial, spectral, and noise limitations are imposed by the sensor itself (e.g., Yamano and Tamura 2004; Kendall and Miller 2008); and (3) similarities between the reflectance of the desired substrates may cause errors in their identification (e.g., Hedley

Communicated by Geology Editor Prof. Bernhard Riegl

T. Caras (✉) · A. Karnieli
The Remote Sensing Laboratory, Jacob Blaustein Institutes for Desert Research, Ben-Gurion University of the Negev, Sede-Boker Campus, 84990 Beersheba, Israel
e-mail: divething@yahoo.com

Published online: 30 March 2013

et al. 2004; Knudby et al. 2007). These three limitations are detailed below.

Unlike terrestrial substrates, marine substrates are limited in their available spectral range to somewhere between 400 and 700 nm, dependent on water quality and clarity (e.g., Smith and Baker 1981; Pope and Fry 1997; Zheng et al. 2002). Predominantly, the effect of the water column is that it scatters the shorter wave section of the spectrum (up to about 450 nm) and absorbs most of the available light above 600 nm (e.g., Lee et al. 1999; Woźniak et al. 2010). Understanding the effects of water and their correction is a formidable challenge and has been the subject of numerous studies; these complexities and their potential solutions are beyond the scope of this paper. Regardless, within the spectral range available through water, spectral features are concentrated between 550 and 700 nm (e.g., Hedley and Mumby 2002; Kutser et al. 2003; Hochberg et al. 2006). Furthermore, it is important to note that even with a good water correction procedure, the analysis is confined to a maximum of 3–6 m water depth, beyond which very little light above 600 nm leaves the water (Kutser et al. 2003; Hedley et al. 2010).

Another environmental effect caused by the air–water interface is the glint. This element is dependent on lighting directionality in relation to the sensor position and therefore is often referred to as specular reflection (Kay et al. 2009). Glint can be produced by waves or wavelets that, in a micro-scale, can change the water surface angle, thereby producing a localized glint-like effect. In affected samples (pixels or areas in the image), the reflection measured is significantly higher than other (e.g., neighboring) samples. The correction for glint is relatively simple and is based on normalizing effected pixels to unaffected pixels using a none-water-penetrating wavelength in the near-infrared (NIR) spectral range (Hochberg et al. 2003a; Hedley et al. 2005; Kay et al. 2009).

Spatial resolution (i.e., pixel, the size of the land covered by each remotely sensed unit) and spectral resolution (the number of spectral bands and their width) are usually limited by the ability of the sensor to collect enough energy (Mather and Koch 2004). Put together, even without the effect of water absorbance, the total available radiance (reflected light from the substrate) has to be balanced or optimized between the unit area (pixel) and the number of bands. To this end, with the available technology, it is virtually impossible to achieve both high spectral resolution and high spatial resolution. Therefore, to date, anyone who aims to study the reef using remote sensing has essentially to choose between high spatial resolution (with low spectral resolution) and high spectral resolution (coupled with low spatial resolution). The choice in this dilemma is fundamentally dependent on the scientific task at hand.

A coral reef is a highly heterogeneous habitat in which even the finest spatial resolution available (1–4 m) from spaceborne systems is unlikely to contain a single substrate (Andrefouet et al. 2002; Hochberg and Atkinson 2003; Leiper et al. 2012). Not having a single substrate in a pixel makes the classification infinitely more difficult as the combination of substrates present may not necessarily be linearly contributing to the pixel's reflection (Joyce and Phinn 2002; Hedley 2004). Studies attempting to address this problem have used a combination of solutions such as sub-pixel analysis (e.g., Hedley et al. 2012), or limiting classification resolution to specific highly detectable substrates, such as bleaching (Wooldridge and Done 2004; Dekker et al. 2005; Dadhich et al. 2012). Many of the solutions suggested above can be undertaken only with a high spectral resolution that, in turn, limits the worker to a coarser spatial resolution (from tens of meters upwards) (Sterckx et al. 2005; Kutser et al. 2006; Hedley et al. 2012).

Reef substrates' spectral separability is another subject that has drawn considerable attention (e.g., Hochberg et al. 2003b; Lee et al. 2007; Leiper et al. 2012). Most examples for spectral analysis rely on the benefits of hyperspectral resolution and the ability to detect unique spectral features of pure substrate measurements (e.g., Hochberg et al. 2003b; Karpouzli et al. 2004; Hamylton 2009). Examples of coral reef pure substrate spectra are usually in situ sampling using a hand-held spectrometer (Holden and LeDrew 2002; Wettle et al. 2003). To date, only Hochberg and Atkinson (2000) have used practically pure pixels for their aerial remote sensing analysis despite pixel size of 0.5–0.9 m. This was possible because the substrate unit and area coverage were very homogeneous and do not represent a typical case study for habitats such as coral reefs.

An alternative for coral reef remote sensing is in situ digital photography. Taken underwater or above, it can provide very high spatial resolution (unmatched compared with remote sensing) but provides only three bands. Although these are highly accurate pure pixel images, their analysis is limited by the minimal spectral resolution. Therefore, a typical data analysis of digital photography requires lengthy manual post-processing and is manpower intensive for large-scale coral reef monitoring (English et al. 1997). That said, the potential for extracting high-quality quantitative data, such as species identification or accurate percent cover, could be good if the worker is well trained and manpower is not limited.

Recent developments in sensor production provide innovative remote sensing solutions tested in this study for the first time. The use of a hyperspectral camera from the surface offers an opportunity to deliver a potential solution for all three sources of error discussed earlier: (1) Water correction can be addressed by placing white reference

targets within the image (atmospheric correction is unnecessary) (Mather and Koch 2004); (2) the hyperspectral camera is very similar to the AISA Eagle aerial sensor, featured with the same spectral resolution and up to 80 bands within the relevant range. This spectral resolution far exceeds the resolution recommended for coral reef determination (e.g., Lubin et al. 2001; Hochberg et al. 2003b; Kutser et al. 2003). While this spectral resolution exists in other aerial sensors such as AISA Eagle and CASI, the special resolution is unmatched. Spatial resolution (pixel size) is expected to be finer than that of the target substrate units (e.g., coral colony), thus delivering a pure substrate spectrum in each pixel (much like a digital image); and (3) the combination of high spectral and high spatial (pure pixels) resolution would allow superior recognition of underwater substrates, leading to accurate quantitative estimates of cover within the sampled area (the image). To date, hyperspectral imaging data of this type have never been used in the shallow marine environment. Therefore, it resembles a combination of a field point spectrometer that provides hyperspectral resolution and a digital camera that produces high spatial resolution. Using the proposed technology may lead to the development of an image acquisition and processing system that enables the analysis of the reef features in a fast, accurate, and efficient way. An advanced and improved design will support a semi-automatically run system with minimal operator input over larger areas. All these reasons together formed a strong rationale for testing the capabilities of the proposed technology.

The aim of this study was to provide a preliminary assessment of ground-level, above-water, remote sensing of a coral reef. The objectives include acquiring a hyperspectral image, correction of environmental distortions, and classification of the underwater substrates. In line with the aim, the key objective is achieving the best (most accurate) classification for the given image, using only basic processing steps. Given the pioneering level of processing protocol, objectives included testing a variety of variables relevant to image preprocessing, including spectral resolution and spectral ranges.

Methods

Study site

The coral-reef marine park (CRMP, 29°33′N 34°57′E) is located at the northern end of the Gulf of Aqaba, 8 km south of the city of Eilat, Israel. The study site is categorized as fringing reef and is relatively small while the reef table is approximately 25 m wide and 2 km long. The choice of location is based on the availability of an overwater dry structure and the relatively flat reef table.

Image acquisition

The hyperspectral image was obtained from the jetty (bridge) over the reef (Fig. 1). Time to provide the best results, the image was acquired during the late morning—when the sun was at an angle that avoided glint effect. Other conditions included low wind (approximately 5 knots), and the water was close to low tide, so the average depth was 30 cm (ranging from 20 to 50 cm). The camera/instrument used was a pushbroom line scanner Spectral Camera HS by Specim Systems. It was fixed on a boom, overhanging the reef as close as possible to the nadir position. The camera's 28° lens, opening at 2.5 m above target, captured approximately 2 × 3 m of the reef table, and the acquisition time was near 32 s. The camera provides 1,600 pixels per line (the image width); therefore, divided by 2 m of image width, it gives, on average, 1.25 mm of reef substrate area per pixel. Lengthwise, the camera is able to provide up to 2,500 lines although only 1,400 of those were captured to minimize image distortion at the edges. Spectrally, 849 bands are captured in the spectral range of 400–1,000 nm with a 0.67–0.74 nm band width.

For demonstrating the technique, a subset of 500 × 500 pixels was selected from the entire image in order to minimize pixel stretching due to camera angle (Fig. 2a, b). The image included a plastic quadrate frame and two white reference plates—one at the reef table depth (Fig. 2a) and another at the water surface (not shown).

Image preprocessing and analysis

A digital number (DN) is a value assigned to a pixel in a digital image that depicts the average radiance of the basic

Fig. 1 The construction of the hyperspectral camera on the bridge. At this fully extended boom height, the camera can cover 3 × 6 m of reef

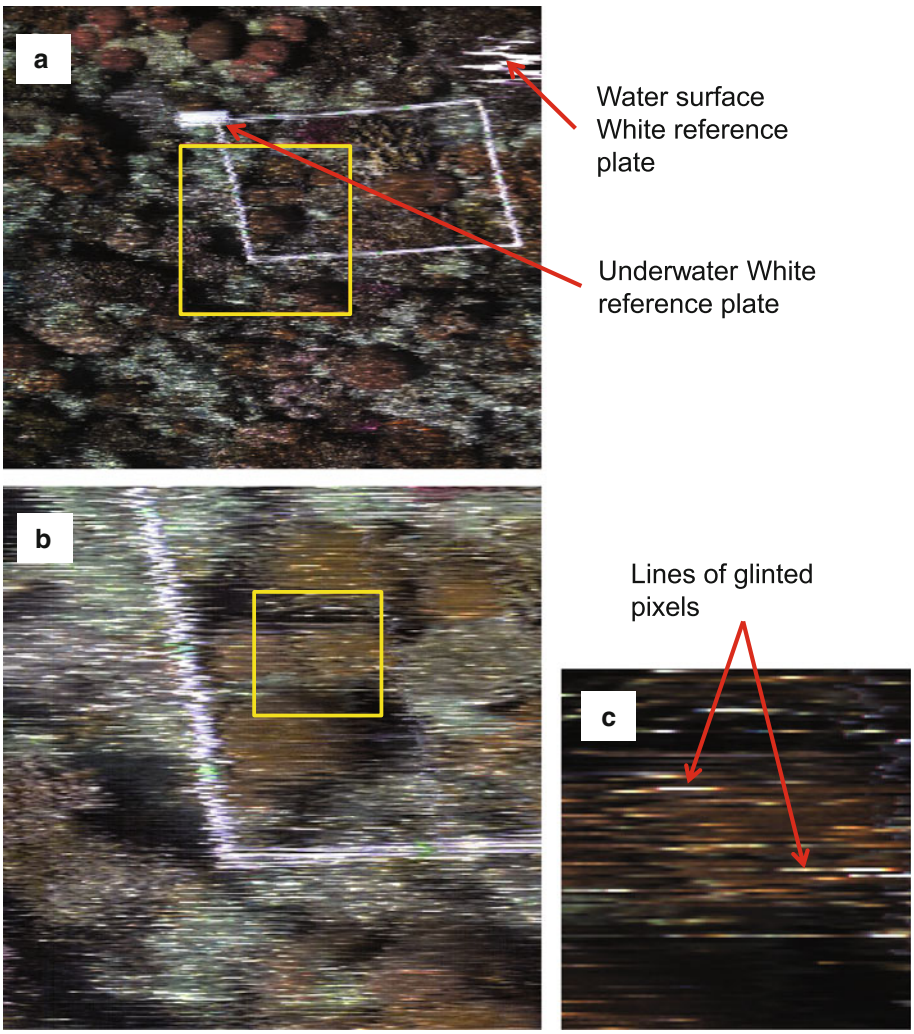

Fig. 2 An example of a hyperspectral image. **a** the original full size image; **b** a clip used for all analyses; and **c** a close-up section showing glinted (*under the cross*) and non-glinted pixels

picture element (pixel). The white reference needed for water correction was an extracted spectrum of the underwater white reference plate placed within the image at the reef depth. Dividing the DN values by those of the white reference converts all irradiance values into reflectance values completing the image preparation (Lillesand and Kiefer 2003; Mather and Koch 2004). Measuring that plate underwater offers an opportunity to correct the effect of the water medium on light passing through. This is based on the assumption that—just like on land—those plates provide a baseline measurement representing all the light that can be reflected from the target in those conditions. Since the image analysis is undertaken in reflectance values and the correction was based on an image-derived white reference, radiometric correction is an unneeded step and was omitted from the image preparation sequence. Altogether, three images were created to test the spectral resolution parameter. The original image was spectrally resampled to three spectral resolutions: 5 nm bands, 10 nm bands, and 20 nm bands, reducing the original number of bands between 400 and 800 nm to 80, 40, and 20, respectively.

The final step of the pre-processing focused on addressing the severe variability in spectral albedo, including the glinting effects caused by surface ripples (Fig. 2c). Those glinted pixels were different from their surrounding pixels, both by their reflectance magnitude and by their spectral features in the NIR spectral range (Fig. 3a). Instead of filtering out high albedo pixels and imposing a uniform correction approach on the darker pixels as well as the light ones, a normalization procedure was employed. This processing adopted the deglinting method described by Hochberg et al. (2003a) and Hedley et al. (2005). This correction is based on using the water opacity in the NIR wavelengths (thus reflectance values are independent of water absorption) as a baseline for normalization. In this respect, it is similar to more familiar normalization techniques based on the mean or mode of all bands. In the first stage of this routine, each band is divided by a specific near-

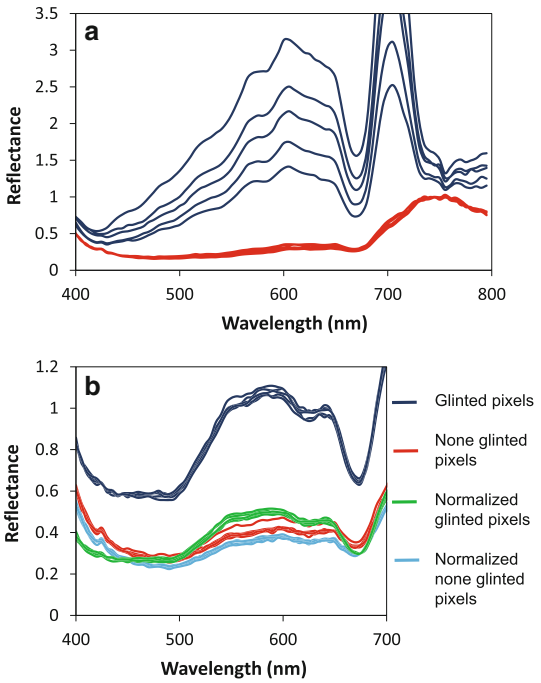

Fig. 3 Glinted and non-glinted spectra of massive coral and their normalization. After conversion to reflectance, the *Y* axis represents the fraction of reflectance from the maximum, and their values should range between 0 and 1 (i.e., *white* reference should reach one). Spectra that are over the value of one suggest that they are overexposed as result of glinting effect. **a** While spectra of branching coral tend to be fairly consistent in their albedo, glinted spectra (*blue*) are more varied and their spectral features not consistent beyond 700 nm. **b** Spectra of glinted massive hard coral before and after normalization. Shown here are also non-glinted pixels before and after normalization. Note that normalization affects albedo without affecting the spectral features themselves

infrared (NIR) band (not specified). The second stage of this method suggests normalizing all pixels to a certain minimum value originally termed NIR min but referred to as 'min' from here on. The min value is derived from non-glinted pixels selected manually by the operator. In this step, the linear relationship, created earlier, is reversed by simple multiplication using the new min value (instead of the original NIR band used for division). The output is an image where all pixels in the image have a uniform baseline based on the min derived from a non-glinted pixel.

Theoretically, glint correction should come in earlier stages of preprocessing, prior to reflection conversion, as the glinted pixels contain reflection spectra that did not enter the water column (reflected from the surface directly) at all. However, in this case, because the 'deglinting' approach is used only as a normalization agent, the introduced bias is ignored. The leading rationale in this choice was that any bias is applied to all spectra and since it is derived from the image itself, its effect is uniform across the image. Moreover, since classification training is also based on the same biased within-image spectra, the classification itself is not affected by their radiometric incorrectness. Additionally, the most affected part of the spectrum would be in the NIR—an area of the spectrum not taking part in the classification anyway. The normalization procedure tested four bands based on the above method. In the first stage, each spectrum was expressed as a proportion to one of the following bands (red bands: 675, 680 and NIR bands: 760 and 775 nm). The two red bands were chosen since they represented an area in the spectrum that is typical to a living substrate (i.e., typical chlorophyll absorption peak at 675 nm) and also because their standard deviation was the smallest in the image. The NIR section bands were chosen based on low standard deviation alone following Hedley et al. (2005). Next, the images were multiplied by 0.3, the average reflection of bands 675 and 680 nm in well-lit pixels (i.e., pixels that are not affected by glint or shade). A similar process took place for the NIR-divided images that were multiplied by 0.92. The resulting normalized images were used for classification.

The general spectral range of water-leaving radiance suggested in the literature is 400–700 nm. From this range, two sets of spectral ranges were selected based on close observation of the spectra in the image and the following rationale. Due to a combination of high light scattering and the lack of useful spectral features (e.g., Lubin et al. 2001), the spectral range between 400 and 450 nm was omitted. The spectral range between 650 and 700 nm is highly affected by water absorption but does contain important spectral features, like the chlorophyll absorption peak at 675 nm. Because omitting this range may affect the separability of tested substrate, two spectral ranges were selected to represent the spectral range options 450–650 nm and 450–700 nm.

Image classification

Image classification was applied using support vector machine (SVM), a standard supervised classification procedure in ENVI software. SVM is based on modeling the training classes in hyperspace and minimizing each pixel's distance to its most similar target. The SVM enables one to seek those distances in a nonlinear way (Cortes and Vapnik 1995) and is particularly effective with spectral data.

Image classification focused on five classes: massive hard coral, branching hard coral, deeper turf rock, shallow turf rock, and shade. For every identified class, 10 adjacent pairs of areas of interest (AOI) were selected; each AOI contained in excess of 250 pixels (therefore, each class average was based on more than 2,000 pixels). Adjacent AOIs were expected to contain pixels of the same class, so one of every pair was allocated for classification training while the second AOI was later used for verification (Fig. 4). Altogether, classification was undertaken ten

times: There were five images, including the original image, two red-band-normalized images and two NIR-band-normalized images; each of those was classified twice using the two spectral ranges 450–650 nm and 450–700 nm. Confusion matrices, calculated from the resulting classed images, offered a quantitative assessment for the success of the classification in each image. Two measurements for accuracy were calculated—total accuracy, representing the number of correct classifications as a fraction of the total, and the Kappa coefficient, representing accuracy that takes into account classification occurring by chance.

Results

Deglinting

Deglinted pixels were only a small proportion of the entire image (~3 %), and their effect ranged from saturated pixels (i.e., after white reference correction, pixels contained values larger than 1) to over-lit pixels (Fig. 3a). It seems that due to the sensor's pushbroom action, glint was, in many cases, recorded in lines. The key for the normalization success was assumed to be in choosing the right band on which to base the correction and from which to extract the 'min' values. Although spectrally biased, both correction procedures produced an improved spectral image where much of the within-substrate unit variability (shade or glint) was reduced without losing useful spectral features (Fig. 3b).

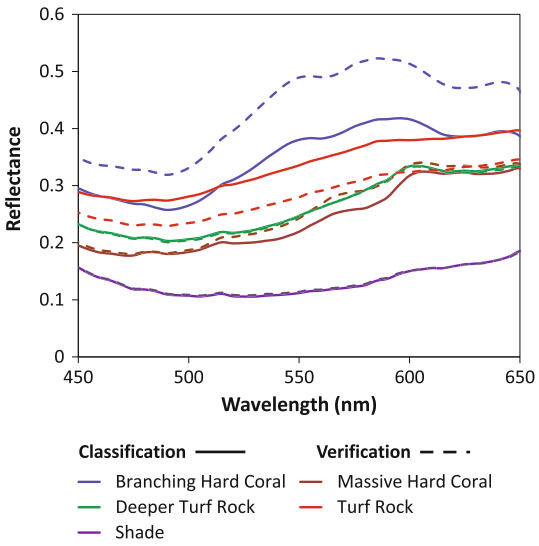

Fig. 4 Spectra used for classification. The *solid lines* represent the average spectra used for classification while the *dashed line* is the average spectra of the verification areas of interest. The classes include branching hard coral, massive hard coral, turf rock, rock, and shade. Note that while the albedo is not always identical, spectral features are similar

Classification

Overall, the most accurate classification was achieved using the combination of 5 nm bands, a 450–660-nm range, and red-band normalization (total accuracy was 0.99 and Kappa coefficient was 0.99, Table 1). Of the five images tested, the two images corrected with NIR bands (765 and 775 nm) and the two images corrected with the red bands (675 and 680 nm) produced identical accuracies (not presented). Out of the two spectral ranges, the wide spectral range (450–700 nm) gave better results than that of the narrow spectral range (450–650 nm). The exclusion to the above rule was the red-band corrections that were generally improved using the narrower spectral range and narrower bands. Both normalization treatments improved the classification in comparison with that of the original image although red-band normalization consistently produced more accurate results (e.g., 0.99 for red versus 0.9 for NIR-corrected bands classified between 450 and 650 nm bands and 5 nm band width). Overall accuracy scores for all the tested images and the corresponding Kappa coefficient scores were highly correlated (R^2 = 0.99).

Throughout, despite the normalization, severely glinted spectra and very dark spectra were more likely to be misclassified or unclassified. Normalization improved the micro-scale—within colony—classification (Fig. 5) for both high albedo (glint) and low albedo (shade) pixels. For example, the spherical coral shade is classified as 'shade' (or unclassified) in the original image, while correctly identified as 'coral' in the normalized images. In all cases, class perimeter is better defined after normalization that improves the identification of turf areas significantly (Fig. 6).

Discussion

The results presented in this preliminary study suggest that ground-level hyperspectral imagery can be used successfully to classify coral reef substrates. Furthermore, the addition of normalization significantly increases classification accuracy. Despite the fact that the red-band normalization is radiometrically biased, it achieves better accuracy than that of the NIR band because the classification endmembers and the classified pixels are subjected to the same treatment. This may have to be addressed if classification were to rely on external data, such as a spectral library or endmembers derived from another image. Using a different form of normalization may improve accuracy without imposing bias limitations and also may allow cross referencing between images (Roger et al. 2003). In contradiction to previous work where normalization was not used (e.g., Lubin et al. 2001; Kutser

Table 1 Confusion matrix results of the most successful image classification tested (5 nm bands, 450–660 nm range, and red-band normalization)

Confusion matrix	Verification				
	Branching hard coral	Massive hard coral	Turf rock	Deeper turf rock	Shade
Classification					
Branching hard coral	388	0	0	0	0
Massive hard coral	0	849	2	2	0
Turf rock	1	2	492	0	5
Deeper turf rock	7	0	0	258	0
Shade	0	0	12	0	802

The total accuracy was 0.99 and Kappa coefficient was 0.99

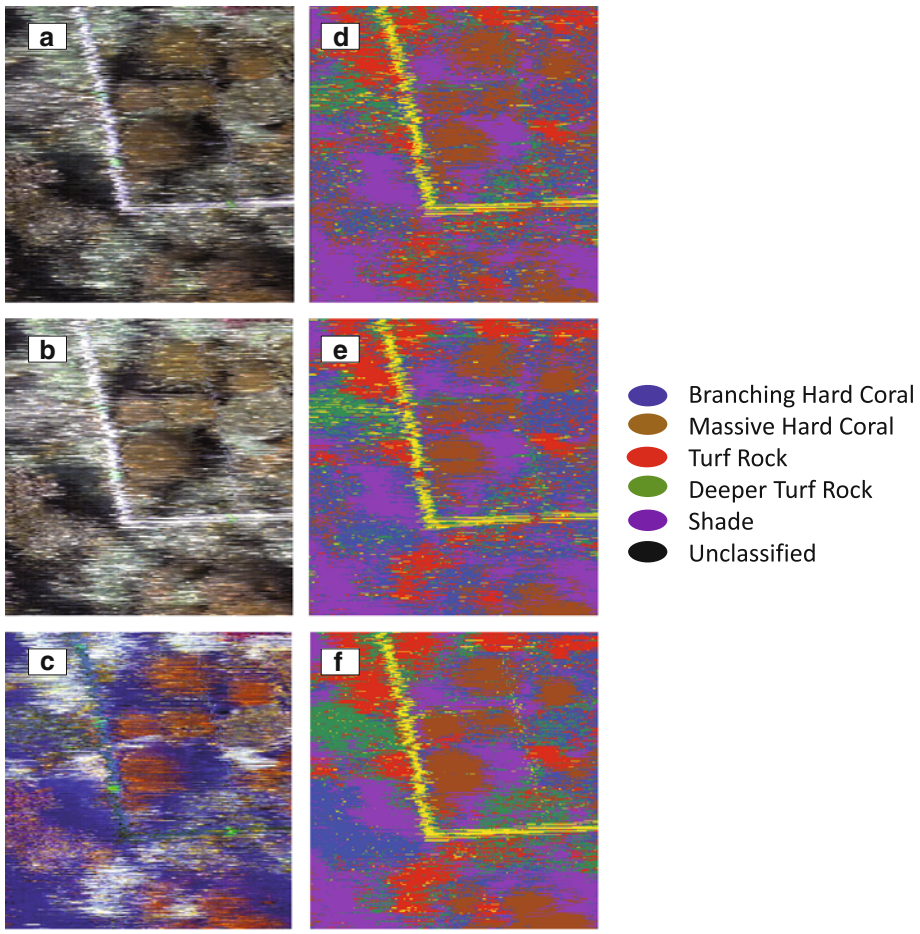

Fig. 5 Deglinting and classification results. **a**–**c** are the images before normalization, after NIR-band normalization, and after red-band normalization, respectively. The *marked areas* of interest (AOI) in the image represent the training and verification AOIs used for the classification process. *Color legend* follows previous colors (Fig. 3). **c**–**e** are the classified images. **c** is the non-deglinted image; **d** is the classified deglinted image; and **e** is the normalized. Accuracy in classification is visually noticed

et al. 2003), spectral resolution or spectral range limitations did not seem to have played an important role in improving accuracy. The SVM is a practical tool in extracting a classification model when the data are noisy or when the spectra are not well defined, such as marine substrates (Cortes and Vapnik 1995; Kruse 2008). As a classification approach, it is somewhat similar to the principal component analysis (PCA) that was suggested by previous workers as a good method of maximizing the benefit of high spectral resolution data sources (e.g., Holden and LeDrew 1998; Hochberg and Atkinson 2003; Hedley et al. 2012).

If we consider that the remote sensing of coral reefs suffers from additional drawbacks in comparison with terrestrial equivalents, using the hyperspectral camera over the reef table seems to overcome these limitations well (environmental, sensor, and habitat). The first, and in many cases the hardest, to encounter is the environmental problem of water scattering and absorption. The use of an in situ white reference plate used in this study was found to

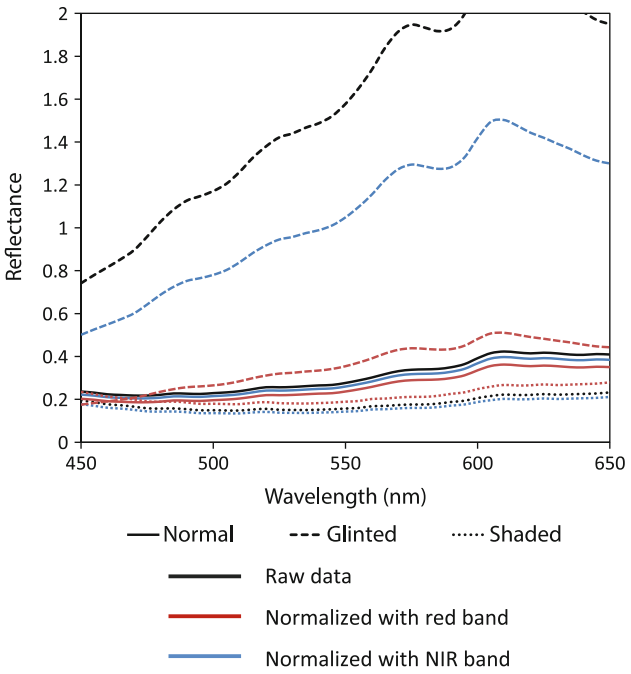

Fig. 6 A demonstration of spectra treatment results. The *solid lines* represent the average lit spectra. The *dashed lines* and the *dotted lines* represent glinted and shaded spectra, respectively. Raw (untreated) coral pixels are in *black*, pixels normalised with *red* band in *red*, and coral pixels normalised with NIR band pixels in *blue*

be useful in the reef table conditions especially in omitting the need for water correction. In this respect, water quality and water type (Jerlov 1951) are not considered, and water correction is not necessary (Lee et al. 1999). The success of this option is currently tested for deeper water and will be applied in different conditions. Another environmental, water-related drawback is the distortion caused by glint (Kay et al. 2009). This element seemed to be overcome successfully by using a simple correction procedure in two variations.

The second limitation, imposed by the sensor itself, is the camera's most significant merit. Even the finest-scaled remote sensing image pixel exceeds substrate unit sizes (e.g., pixels size may be 1 m but average coral heads at the study site may range to around 25 cm in diameter). The hyperspectral camera provides millimeter-scale pixels, an impressive spatial scale allowing all of the pixels in the image to contain a single substrate. In fact, both resolution elements (spectral and spatial) offered by the sensor used here are well over the minimum needed to execute marine substrate classification successfully (Hochberg et al. 2003b; Kutser et al. 2006; Knudby et al. 2010).

The final difficulty outlined earlier is the similarity between the different reef living-substrate spectra as they are all dominated by the same chlorophyll absorption features. Hyperspectral imagery is probably the only means for addressing the feature separation necessary for positive identification of different marine substrates (Kutser and Jupp 2006; Leiper et al. 2012). The spectral resolution of the camera used for this study provides adequate spectral resolution to successfully separate the common substrates within the study site.

Bridging the technological capabilities between remote sensing and in situ spectroscopy offers a good opportunity for testing resolution limitations. Starting off at the fine resolution offered by this sensor, reducing the spectral resolution by resampling the same data set may facilitate further investigation into the limits of the spectral resolution parameter.

The ability to provide pure pixels offers an opportunity to run a simple classification on the selected scene, an uncommon option for in situ analysis of marine substrates (Hochberg and Atkinson 2003). Furthermore, results presented here suggest that sub-classification to branching hard coral (e.g., *Acropora* spp.) and massive hard coral (e.g., *Platygyra* spp.) was also possible, a novel applicability not possible to date. To this end, even pixels of a few centimeters (and tenfold upscale!) would provide a very useful classification and quantification data set. The potential for testing the effect of spatial up-scaling may help in optimizing the remote sensing effort in future research (Andrefouet et al. 2002; Purkis and Riegl 2005; Dadhich et al. 2012). In contrast, the combination of micro-scale pure pixels and high spectral resolution provides an exciting opportunity to investigate and address within-class variability, such as shading and the 3D complexity of marine substrates. Understanding these effects can help explain the spectral nonlinear mixing described by several studies that attempted to perform these tasks (Hedley and Mumby 2003; Goodman and Ustin 2007; Bioucas-Dias and Plaza 2010). At this scale, models of classification can test approaches in contextual classifications (Mumby et al. 1998; Vanderstraete et al. 2005), textual classifications (Mumby and Edwards 2002; Riegl and Purkis 2005; Purkis et al. 2006) or object recognition techniques (Gilbes et al. 2006; Phinn et al. 2011; Leon et al. 2012). Particularly important is the sharper substrate unit edges obtained using the red-band normalization. Being able to identify and isolate different units in the scene is a major step-up in object recognition processing (Gilbes et al. 2006).

With all this in mind, it is important to remember that the pushbroom technology poses a problematic limitation—the exposure time. Even if the current exposure time can be reduced by decreasing spectral resolution, the instrument currently used has to be fixed to a static base. To date, there is no reflex camera alternative although the technology is being developed (FluxData; SurfaceOptics-Corporation; Habel et al. 2012).

For monitoring and conservation, the potential applications demonstrated by this study include automated quantitative image analysis and accurate substrate identification. In turn, this facilitates larger scale campaigns (i.e., multiple image analysis) with much less manpower investment, compared to knowledge-based digital photography analysis. The immediate applicability is currently limited by the need for camera mounting (such as a tripod or the jetty used for this study). This may be overcome using a reflex-type camera as described earlier but could be also overcome by using a higher mounting for the current sensor. For example, raising the sensor to 6 meter above the reef may cover an extended portion of the reef, approximately 3 m × 6 m (effectively spatial up-scaling). In this case, the spatial resolution will be reduced but that is unlikely to affect the image analysis. Even with all the current limitations, for the study site described in this study—using the two jetties to take 5 images at each side would result in a set of 20 images. If, as suggested above, every image covers 18 m^2, this amounts to a sizable survey effort.

The aim of this paper was to give a quick and simplified account of the potentiality of a new technology for marine spectroscopy at ground level. The three key limitations relevant to remote sensing of coral reefs are successfully overcome. The presented results show that the combination of image specification 5 nm bands, a 450–660 nm range and the red-band normalization can produce unprecedented classification accuracies of 99 %. To this end, the camera's specifications open a new avenue of research in the spectroscopy, image analysis, and remote sensing relevant to this environment. The advantage of such resolution is limited in respect to computer power and data handling. To overcome this problem, currently the possibility of reducing spatial and spectral resolution is being tested. Up-scaling experiments may provide resolution limits for this type of remote sensing analysis of coral reefs. Scaling up the area surveyed can be done empirically by rising the sensor's mounting point and by creating mosaics of several images together. Another area in need of improvement is the normalization technique that currently is image specific. Further work planned for this source of imagery focuses on testing different normalization techniques. The results presented here show how well the classification handles a relatively simple scene with only five class definitions. In more complex scenes, the number of classes may be doubled, and class integrity may be reduced. Tests with more complex classification techniques, such as PLS-DA and object recognition, are planned and may yield better results with more complex scenes. Additional avenues for exploration include micro-scale (single colony) spectral variation and spatial up-scaling of similar images.

References

Andrefouet S, Berkelmans R, Odriozola L, Done T, Oliver J, Muller-Karger FE (2002) Choosing the appropriate spatial resolution for monitoring coral bleaching events using remote sensing. Coral Reefs 21:147–154

Bioucas-Dias J, Plaza A (2010) Hyperspectral unmixing: Geometrical, statistical and sparse regression-based approaches. SPIE Remote Sensing Europe, Image and Signal Processing for Remote Sensing Conference

Collin A, Planes S (2012) Enhancing coral health detection using spectral diversity indices from WorldView-2 Imagery and Machine Learners. Remote Sens 4:3244–3264

Cortes C, Vapnik V (1995) Support-vector networks. Machine Learning 20:273–297

Dadhich AP, Nadaoka K, Yamamoto T, Kayanne H (2012) Detecting coral bleaching using high-resolution satellite data analysis and 2-dimensional thermal model simulation in the Ishigaki fringing reef, Japan. Coral Reefs 31:425–439

Dekker AG, Wettle M, Brando VE (2005) Coral reef habitat mapping using MERIS: can MERIS detect coral bleaching? MERIS (A)ATSR Workshop 2005 Published on CDROM:25.21

English S, Wilkinson C, Baker V (1997) Survey manual for tropical marine resources. Australian Institute of Marine Science, Townsville

FluxData I The FD-1665-MS 7 Channel Camera

Gilbes F, Armstrong RA, Goodman J, Velez M, Hunt S (2006) Censsis seabed: diverse approaches for imaging shallow and deep coral reefs. Proceedings of Ocean Optics XVIII

Goodman JA, Ustin SL (2007) Classification of benthic composition in a coral reef environment using spectral unmixing. J Appl Remote Sens 1:011501. doi:10.1117/1.2815907

Habel R, Kudenov M, Wimmer M (2012) Practical spectral photography. Eurographics 2012

Hamylton S (2009) Determination of the separability of coastal community assemblages of the Al Wajh Barrier Reef, Red Sea, from hyperspectral data. European J Geosci 1:1–11

Hedley J (2004) Spectral unmixing of coral reef benthos under ideal conditions. Ph.D. thesis, University of Exeter, pp 108–149

Hedley JD, Mumby PJ (2002) Biological and remote sensing perspectives of pigmentation in coral reef organisms. Adv Mar Biol 43:277–317

Hedley JD, Mumby PJ (2003) A remote sensing method for resolving depth and subpixel composition of aquatic benthos. Limnol Oceanogr 48:480–488

Hedley J, Mumby P, Joyce K, Phinn S (2004) Spectral unmixing of coral reef benthos under ideal conditions. Coral Reefs 23:60–73

Hedley JD, Harborne AR, Mumby PJ (2005) Simple and robust removal of sun glint for mapping shallow-water benthos. Int J Remote Sens 26:2107–2112

Hedley J, Roelfsema C, Phinn SR (2010) Propogating uncertainty through a shallow water mapping algorithm based on radiative transfer model inversion. Ocean Optics XX

Hedley JD, Roelfsema CM, Phinn SR, Mumby PJ (2012) Environmental and sensor limitations in optical remote sensing of coral reefs: Implications for monitoring and sensor design. Remote Sens 4:271–302

Hochberg EJ, Atkinson MJ (2000) Spectral discrimination of coral reef benthic communities. Coral Reefs 19:164–171

Hochberg EJ, Atkinson MJ (2003) Capabilities of remote sensors to classify coral, algae, and sand as pure and mixed spectra. Remote Sens Environ 85:174–189

Hochberg EJ, Andrefouet S, Tyler MR (2003a) Sea surface correction of high spatial resolution Ikonos images to improve bottom mapping in near-shore environments. IEEE Transactions on Geoscience and Remote Sensing 41:1724–1729

Hochberg EJ, Atkinson MJ, Andrefouet S (2003b) Spectral reflectance of coral reef bottom-types worldwide and implications for coral reef remote sensing. Remote Sens Environ 85:159–173

Hochberg EJ, Appril A, Atkinson MJ, Bidigare RR (2006) Bio-optical modeling of photosynthetic pigments in corals. Coral Reefs 25:99–109

Holden H, LeDrew E (1998) Deconvolution of measured spectra based on principal components analysis and derivative spectroscopy. Geoscience and Remote Sensing Symposium Proceedings, 1998. IGARSS '98. 1998 IEEE International 2:760–762

Holden H, LeDrew E (2000) Optical water column properties of a coral reef environment: towards correction of remotely sensed imagery. Geoscience and Remote Sensing Symposium, 2000. Proceedings. IGARSS 2000. IEEE 2000 International 6:2666–2668

Holden H, LeDrew E (2002) Hyperspectral linear mixing based on in situ measurements in a coral reef environment. Geoscience and Remote Sensing Symposium, 2002. IGARSS '02. 2002 IEEE International 1:249–251

Jerlov NG (1951) Optical studies of ocean water. Report of Swedish Deep-Sea Expeditions 3:1–59

Johansen K, Roelfsema C, Phinn S (2008) High spatial resolution remote sensing for environmental monitoring and management preface. J Spatial Sci 53:43–47

Joyce KE, Phinn SR (2002) Bi-directional reflectance of corals. Int J Remote Sens 23:389–394

Karpouzli E, Malthus T, Place C (2004) Hyperspectral discrimination of coral reef benthic communities in the western Caribbean. Coral Reefs 23:141–151

Kay S, Hedley JD, Lavender S (2009) Review: Sun glint correction of high and low spatial resolution images of aquatic scenes: a review of methods for visible and near-infrared wavelengths. Remote Sens 1:697–730

Kendall MS, Miller T (2008) The influence of thematic and spatial resolution on maps of a coral reef ecosystem. Mar Geodesy 31:75–102

Knudby A, LeDrew E, Newman C (2007) Progress in the use of remote sensing for coral reef biodiversity studies. Prog Phys Geogr 31:421–434

Knudby A, Newman C, Shaghude Y, Muhando C (2010) Simple and effective monitoring of historic changes in nearshore environments using the free archive of Landsat imagery. Int J Appl Earth Obs Geoinform 12:S116–S122

Kruse FA (2008) Expert system analysis of hyperspectral data. SPIE Defense and Security, Algorithms and Technologies for Multispectral, Hyperspectral, and Ultraspectral Imagery XIV, Conference DS43 6966–25

Kutser T, Jupp DL (2006) On the possibility of mapping living corals to the species level based on their optical signatures. Estuar Coast Shelf Sci 69:607–614

Kutser T, Dekker AG, Skirving W (2003) Modeling spectral discrimination of Great Barrier Reef benthic communities by remote sensing instruments. Limnol Oceanogr 48:497–510

Kutser T, Miller I, Jupp DLB (2006) Mapping coral reef benthic substrates using hyperspectral space-borne images and spectral libraries. Estuar Coast Shelf Sci 70:449–460

Lee Z, Carder KL, Mobley CD, Steward RG, Patch JS (1999) Hyperspectral remote sensing for shallow waters: 2. Deriving bottom depths and water properties by optimization. Appl Opt 38:3831–3843

Lee Z, Carder K, Arnone R, He M (2007) Determination of primary spectral bands for remote sensing of aquatic environments. Sensors 7:3428–3441

Leiper I, Phinn S, Dekker AG (2012) Spectral reflectance of coral reef benthos and substrate assemblages on Heron Reef, Australia. Int J Remote Sens 33:3946–3965

Leon J, Phinn SR, Woodroffe CD, Hamylton S, Roelfsema C, Saunders M (2012) Data fusion for mapping coral reef geomorphic zones: possibilities and limitations Proceedings of the 4th GEOBIA, Rio de Janeiro, pp 261–266

Lillesand TM, Kiefer RW (2003) Remote sensing and image interpretation. John Wiley and Sons, New York

Lubin D, Li W, Dustan P, Mazel CH, Stamnes K (2001) Spectral signatures of coral reefs: Features from space. Remote Sens Environ 75:127–137

Mather PM, Koch M (2004) Computer processing of remotely-sensed images: An introduction. John Wiley and Sons

Mumby PJ, Edwards AJ (2002) Mapping marine environments with IKONOS imagery: enhanced spatial resolution can deliver greater thematic accuracy. Remote Sens Environ 82:248–257

Mumby PJ, Green EP, Clark CD, Edwards AJ (1998) Benefits of water column correction and contextual editing for mapping coral reefs. Int J Remote Sens 19:203–210

Mumby PJ, Skirving W, Strong AE, Hardy JT, LeDrew EF, Hochberg EJ, Stumpf RP, David LT (2004) Remote sensing of coral reefs and their physical environment. Mar Pollut Bull 48:219–228

Phinn SR, Roelfsema CM, Mumby PJ (2011) Multi-scale, object-based image analysis for mapping geomorphic and ecological zones on coral reefs. Int J Remote Sens 33:3768–3797

Pope RM, Fry ES (1997) Absorption spectrum 380–700 nm of pure water. II. Integrating cavity measurements. Appl Opt 36:8710–8723

Purkis SJ, Riegl B (2005) Spatial and temporal dynamics of Arabian Gulf coral assemblages quantified from remote-sensing and in situ monitoring data. Mar Ecol Prog Ser 287:99–113

Purkis SJ, Myint SW, Riegl B (2006) Enhanced detection of the coral *Acropora cervicornis* from satellite imagery using a textural operator. Remote Sens Environ 101:82–94

Riegl BM, Purkis SJ (2005) Detection of shallow subtidal corals from IKONOS satellite and QTC View (50, 200 kHz) single-beam sonar data (Arabian Gulf; Dubai, UAE). Remote Sens Environ 95:96–114

Roger JM, Chauchard F, Bellon Maurel V (2003) EPO - PLS external parameter orthogonalisation of PLS application to temperature-independent measurement of sugar con-tent of intact fruits. Chemometrics and Intelligent Laboratory Systems 66:191–204

Smith RC, Baker KS (1981) Optical properties of the clearest natural waters (200–800 nm). Appl Opt 20:177–184

Sterckx S, Debruyn W, Vanderstraete T, Goossens R, Van der Heijden P (2005) Hyperspectral data for coral reef monitoring. A case study: Fordate, Tanimbar, Indonesia. EARSeL eProceedings 4(1):18–25

SurfaceOpticsCorporation SOC700Hz/SOC760 Real-time Hyperspectral (HS) Imager

Vanderstraete T, Goossens R, K. GT (2005) Coral reef habitat mapping in the Red Sea (Hurghada, Egypt) based on remote sensing. EARSeL eProceedings 3(2):191–207

Wettle M, Ferrier G, Lawrence AJ, Anderson K (2003) Fourth derivative analysis of Red Sea coral reflectance spectra. Int J Remote Sens 24:3867–3872

Wooldridge S, Done T (2004) Learning to predict large-scale coral bleaching from past events: A Bayesian approach using remotely sensed data, in-situ data, and environmental proxies. Coral Reefs 23:96–108

Woźniak SB, Stramski D, Stramska M, Reynolds RA, Wright VM, Miksic EY, Cichocka M, Cieplak AM (2010) Optical variability of seawater in relation to particle concentration, composition, and size distribution in the nearshore marine environment at Imperial Beach. California. J Geophys Res 115:C08027

Yamano H, Tamura M (2004) Detection limits of coral reef bleaching by satellite remote sensing: Simulation and data analysis. Remote Sens Environ 90:86–103

Zheng X, Dickey T, Chang G (2002) Variability of the downwelling diffuse attenuation coefficient with consideration of inelastic scattering. Appl Opt 41:6477–6488